

# Properties of Strangelets at Finite Temperature in Liquid Drop Model \*

Y. B. He<sup>1,2</sup>, C. S. Gao<sup>1,2,3</sup>, X. Q. Li<sup>1,3,4</sup>, and W. Q. Chao<sup>1,3,5</sup>

1. *China Center of Advanced Science and Technology (World Laboratory),*

*P.O. Box 8730, Beijing 100080, China*

2. *Department of Physics, Peking University, Beijing 100871, China*

3. *Institute of Theoretical Physics, Academia Sinica, P.O. Box 2735, Beijing 100080, China*

4. *Department of Physics, Nankai University, Tianjin 300071, China*

5. *Institute of High Energy Physics, Academia Sinica, P.O. Box 918(4), Beijing 100039, China*

(September 18, 2018)

## Abstract

A comprehensive study of the properties of strangelets at zero and finite temperature is presented within the framework of liquid drop model, including the essential finite size effects. Strong parameter dependences of the properties are found and discussed.

12.38.Mh, 12.39.Ba, 25.75.+r, 24.85.+p

Typeset using REVTeX

---

\*Partly supported by the National Natural Science Foundation of China

## I. INTRODUCTION

It was argued by Witten [1] that strange quark matter might be the ground state of normal nuclear matter at zero temperature and zero pressure, which was later supported by the studies of Farhi and Jaffe [2] based on MIT bag model. The existence of stable strange quark matter would have some remarkable consequences in cosmology and astrophysics. For instance, it has been suggested [1] that some of the dark matter in the Universe could possibly exist in the form of strange quark matter which was produced when the Universe underwent the quark to hadron transition. The possible transition of a neutron star into a strange star was discussed as well [3,4]. In addition, there have been proposals that the strange stars might be the sources of gamma rays with very high intensities [5,6]. Recently Greiner and his collaborators [7] have proposed that small lumps of strange quark matter (“strangelets”) might be produced in ultrarelativistic heavy-ion collisions, and they could serve as an unambiguous signature for the formation of quark-gluon plasma. In fact, several heavy-ion collision experiments at Brookhaven and CERN are searching for strangelets [8].

Most strange quark matter investigations [2,9,10] have been performed based on shell model or liquid drop model. While calculations in shell model are rather tedious, recently Madsen [11] has pointed out that the general structure of shell model results can be obtained more readily from liquid drop model. On the other hand, strange quark matter at finite temperature has attracted some special interests [12,13], since in some cases, such as ultrarelativistic heavy-ion collisions, strange quark matter is expected to exist in a hot environment. However, these studies of strange quark matter at finite temperature have not completed the treatment of finite size effects, which are expected to play a substantial role in strangelets possibly appearing in the scope of ultrarelativistic heavy-ion collision experiments [14]. The present work is an attempt to apply liquid drop model to strangelets at finite temperature, and could be a step towards the studies of phase structure and evolution of strange quark matter. We will include the important finite size effects (volume, surface and curvature contributions) to study the overall properties of strangelets at finite

temperature, which might give some clues to the search of strangelets.

In the literature [2,11,15] there have been discussions on parameter dependences of the stability of strange quark matter at zero temperature. However, it is interesting as well to study how the parameter “windows” for stable strange quark matter would become, if strange quark matter at finite temperature, *e.g.* strange stars with a temperature up to tens of MeV, is assumed to exist stably in nature. In this work we shall investigate the properties of strange quark matter at finite temperature for a wide range of parameters.

## II. FORMALISM

We consider the strangelet as a gas of up, down, strange quarks, their antiquarks, and gluons confined in an MIT bag. In liquid drop model [11], the grand potential of the system is given by

$$\Omega = \sum_i \Omega_i + BV. \quad (1)$$

Here  $B$  is the bag constant,  $V$  is the bag volume, and the grand potential of particle species  $i$  can be written as

$$\Omega_i = \mp T \int_0^\infty dk \frac{dN_i}{dk} \ln[1 \pm \exp(-(\epsilon_i(k) - \mu_i)/T)], \quad (2)$$

where the upper sign is for fermions, the lower for bosons,  $\mu$  and  $T$  are chemical potential and temperature,  $k$  and  $\epsilon_i$  are particle momentum and energy. In a multiple reflection expansion [16] the density of states is given by

$$\frac{dN_i}{dk} = g_i \left\{ \frac{1}{2\pi^2} k^2 V + f_S^{(i)} \left( \frac{m_i}{k} \right) k S + f_C^{(i)} \left( \frac{m_i}{k} \right) C + \dots \right\}. \quad (3)$$

For spherical strangelets  $V = \frac{4}{3}\pi R^3$  is the volume of the bag,  $S = 4\pi R^2$  is the surface area, and  $C = 8\pi R$  is the extrinsic curvature of the bag surface. The factor  $g_i$  is the statistical weight (6 for quarks and antiquarks, and 16 for gluons).

The surface term for quarks was given by Berger and Jaffe [17] as

$$f_S^{(q)}\left(\frac{m_q}{k}\right) = -\frac{1}{8\pi} \left\{ 1 - \frac{2}{\pi} \arctan \frac{k}{m_q} \right\}, \quad (4)$$

In particular, the surface term for massless quarks and gluons is zero. It has been shown by Madsen [11] that the following ansatz works for the curvature term of massive quarks:

$$f_C^{(q)}\left(\frac{m_q}{k}\right) = \frac{1}{12\pi^2} \left\{ 1 - \frac{3k}{2m_q} \left( \frac{\pi}{2} - \arctan \frac{k}{m_q} \right) \right\}. \quad (5)$$

For gluons the curvature term is [18]

$$f_C^{(g)} = -\frac{1}{6\pi^2}. \quad (6)$$

After the construction of the grand potential as above, we can readily obtain the thermodynamical quantities of the system as follows. The net number of quarks, *i.e.* the number of quarks minus the number of antiquarks, can be derived from

$$N_i = - \left( \frac{\partial \Omega_i}{\partial \mu_i} \right)_{T,V}, \quad (7)$$

and

$$A = \frac{1}{3} \sum_i N_i \quad (8)$$

gives the total baryon number of the strangelet. The free energy  $F$  and internal energy  $E$  of the strangelet are given by

$$F = \sum_i (\Omega_i + N_i \mu_i) + BV, \quad (9)$$

and

$$E = F + TS \quad (10)$$

with the entropy  $S = - \left( \frac{\partial \Omega}{\partial T} \right)_{V,\mu}$ .

### III. NUMERICAL RESULTS

We can study the ground state properties of strangelets at finite temperature  $T$ , *i.e.* the lowest mass state for a given baryon number  $A$  and temperature  $T$ , by minimizing the free

energy  $F$  with respect to the net number of quarks  $N_q$ ,  $N_s$  and the volume of the system  $V$ , at fixed baryon number  $A$ . However, for the sake of illustration, in Fig. 1 we vary the strangeness fraction  $f_s = N_s/A$  (net number of strange quarks per baryon) instead of  $N_s$ , to show the minimum of the free energy per baryon. While the free energy per baryon decreases as temperature rises up from zero to 30 MeV, the value of  $f_s$  which minimizes the free energy per baryon changes little. Actually, as it will be shown later, the strangeness fraction of strangelet in its ground state has weak dependence on temperature.

An easier way to investigate the ground state properties of strangelet is to minimize the free energy analytically with respect to  $N_q$ ,  $N_s$  and  $V$ , under the constraint Eq. (8) for fixed  $A$ , which leads to the mechanical equilibrium condition

$$-\sum_i \frac{\partial \Omega_i}{\partial V} = B, \quad (11)$$

and the optimal composition condition

$$\mu_q = \mu_s \quad (12)$$

(For details see Appendix). Eq. (11) has the explanation that the pressure exerted by the quarks and gluons in the bag is balanced by the bag pressure  $B$ . Eq. (12) might be unexpected, however. It could be interpreted as follows. Since the total number of quarks ( $= N_q + N_s = 3A$ ) in the strangelet is fixed, the free energy of the system is minimized when adding a massless quark (up or down quark) to the strangelet is energetically as favorable as adding a massive strange quark, *i.e.*  $\mu_q = \mu_s$ . Eq. (12) is usually considered as a consequence of bulk strange matter at energy minimum. We argue that Eq. (12) holds for strangelets as long as the liquid drop model is applicable (applicability of liquid drop model to strangelets has been approved by Madsen [11]). Nevertheless, if some other contributions, *e.g.* Coulomb effects, are taken into account, the simple relationship in Eq. (12) will be modified. Eqs. (8)–(12) altogether specify the ground state properties of strangelets.

A strangelet at zero temperature is stable relative to  $^{56}\text{Fe}$  nuclei if its energy per baryon,  $E/A$ , is less than 930 MeV. At finite temperature, however, a strangelet can radiate elementary particles like nucleons and pions from its surface. While it does not lead to the

breakup of a hot strangelet but rather favors the creation of a cold strangelet, pion emission is suppressed at low temperature by a factor  $\sim \exp(-m_\pi/T)$  ( $\sim 0.01$  at  $T=30$  MeV). Furthermore, for a strangelet with  $E/A < 930$  MeV, nucleon emission proceeds via energy fluctuations and will be greatly suppressed [7,12]. If  $E/A > 930$  MeV, on the other hand, nucleon emission process has no threshold and goes much faster, which might drive the hot strangelet to a complete hadronization. Therefore, in this context we shall call a strangelet stable if its  $E/A$  is lower than 930 MeV throughout this work.

In Fig. 2(a) we have presented the (internal) energy per baryon as a function of temperature, for two different baryon numbers,  $A = 20$  and  $100$ , with bag constant  $B^{1/4}=145$  MeV and strange quark mass  $m_s=150$  MeV. Note that the strangelet with a baryon number  $A=100$  is stable only for temperature  $T \lesssim 20$  MeV. (The dot-dashed line in Fig. 2(a) marks an energy per baryon of 930 MeV). We see also that the upper limit of temperature for stable configuration of strangelets depends on baryon number. This is a consequence of the inclusion of finite size effects. More discussions will be given in Fig. 4.

Fig. 2(b)-(d) show the temperature dependence of the strangeness fraction  $f_s$ , charge-to-baryon-number ratio  $Z/A$ , and averaged radius per baryon  $R/A^{1/3}$  of strangelets with  $A=20$ , and  $100$ , for  $B^{1/4}=145$  MeV and  $m_s=150$  MeV. It can be seen that  $f_s$  and  $R/A^{1/3}$  increase, and  $Z/A$  decrease slowly, when the temperature rises up. It is expected that  $f_s$  will saturate to unity, and  $Z/A$  will decrease to zero, when the temperature is high enough, since at that stage the mass difference between up, down and strange quarks is unimportant, the system will tend to become flavor symmetric ( $N_u = N_d = N_s$ ) and globally charged neutral. Our observation of  $Z/A$  as a decreasing function of temperature differs from that of Chakrabarty [13].

In Fig. 3(a)-(d) we have plotted the energy per baryon  $E/A$ , strangeness fraction  $f_s$ , charge-to-baryon-number ratio  $Z/A$ , and averaged radius per baryon  $R/A^{1/3}$  as a function of baryon number  $A$ , for two temperatures  $T=0$  and  $30$  MeV, with  $B^{1/4}=145$  MeV and  $m_s=150$  MeV as well. One can see from Fig. 1(a) that there is a lower limit  $A_{cri}$  to the baryon number of a stable strangelet (whose  $E/A < 930$  MeV). This critical baryon number

is a function of temperature, parameters  $B$  (bag constant) and  $m_s$  (strange quark mass), as will be shown later. Except for sufficiently low baryon number, we see that  $f_s$ ,  $Z/A$  and  $R/A^{1/3}$  depends weakly on  $A$ . Their typical values are  $f_s \simeq 0.4-0.6$ ,  $Z/A \simeq 0.15-0.3$ ,  $R/A^{1/3} \simeq 0.95-1$  fm.

Fig. 4 shows the critical baryon number as a function of temperature, for two different values of  $m_s$ ,  $m_s=150$  MeV (full line) and  $m_s=0$  (dashed line) with  $B^{1/4}=145$  MeV. For temperatures low enough, the critical baryon number increases little. However, beyond some temperature (about 30 MeV for  $m_s=150$  MeV, and 42 MeV for  $m_s=0$ ) even bulk strange quark matter ( $A \rightarrow \infty$ ) could not be stable.

Before any concrete statements can be made, it is reasonable to discuss the parameter dependence. Next we study how the properties of strangelets depend on the two main parameters in liquid drop model, bag constant  $B$  and strange quark mass  $m_s$ .

The variation with  $B^{1/4}$  are plotted in Fig. 5(a)-(d) for strangelets with a baryon number  $A=50$ , at temperature  $T=0$  (full lines) and 30 MeV (dashed lines), with  $m_s=150$  MeV. One can see from Fig. 5(a) that the energy per baryon  $E/A$  is proportional to  $B^{1/4}$  for a given baryon number and temperature. While the strangeness fraction  $f_s$  increases with  $B^{1/4}$ , the charge-to-baryon-number ratio  $Z/A$  and averaged radius per baryon  $R/A^{1/3}$  are decreasing functions of  $B^{1/4}$ .

In Fig. 6 the critical baryon number  $A_{cri}$  is plotted as a function of  $B^{1/4}$ , with the strange quark mass  $m_s=150$  MeV. It can be seen that for sufficiently large bag constant, there could be no stable strange quark matter. This upper limit of  $B^{1/4}$  depends on temperature,  $B^{1/4} \lesssim 153$  MeV at  $T=0$ ,  $B^{1/4} \lesssim 151$  MeV at  $T=15$  MeV, and  $B^{1/4} \lesssim 145$  MeV at  $T=30$  MeV. For strange quark mass less than 150 MeV, the upper limit of  $B^{1/4}$  moves up.

Fig. 7(a)-(d) show the variation with  $m_s$  of properties of strangelets at temperature  $T=0$  and 30 MeV, with baryon number  $A=50$  and  $B^{1/4}=145$  MeV. For strangelets at  $T=0$ , both the energy per baryon  $E/A$  and charge-to-baryon number ratio  $Z/A$  increase with increasing  $m_s$ , and saturate when  $m_s$  reaches the chemical potential  $m_s \simeq \mu_s$ . The strangeness fraction  $f_s$  is a decreasing function of  $m_s$ , and goes to zero when  $m_s \lesssim \mu_s$ . For finite temperature,

$T=30$  MeV, the saturation happens at a larger value of  $m_s$ . However, the averaged radius per baryon  $R/A^{1/3}$  depends little on  $m_s$ .

We have plotted in Fig. 8 the critical baryon number  $A_{cri}$  as a function of  $m_s$ , with  $B^{1/4}=145$  MeV. Note that at zero temperature  $A_{cri}$  increases with increasing  $m_s$ , and suddenly becomes a constant at  $m_s \simeq \mu_s$ , indicating the fact that for  $m_s \lesssim \mu_s$ , no strange quarks exist (see Fig. 7(b) where  $f_s \rightarrow 0$ ), and an increased value of  $m_s$  does not lead to an increase of strangelet energy.

#### IV. DISCUSSIONS AND CONCLUSIONS

In the present work we have neglected QCD radiation corrections, as argued in Refs. [2,17] that an increased value of the strong coupling constant  $\alpha_s$  could be absorbed into a decrease in the bag constant  $B$ . Coulomb effects could be included in liquid drop model self-consistently as shown by Madsen [15]. We show also in Fig. 1 by the dashed lines the free energy per baryon versus strangeness fraction after the inclusion of Coulomb energies. One sees that Coulomb effects are rather negligible for the strangelet energy, but could cause a change of the quark composition of the strangelet (Note in Fig. 1 that the value of  $f_s$  minimizing  $F/A$  is shifted a little by the inclusion of Coulomb effects). The resultant corrections to  $Z/A$  are within the uncertainties caused by parameters  $B$  and  $m_s$ , however.

We have found in this work that the stability of strangelets at zero and finite temperature depends strongly on parameters  $B$ , the bag constant, and  $m_s$ , the strange quark mass. An increased value of  $B$  or  $m_s$  (for  $m_s < \mu_s$ ) tends to destabilize the strangelet. For  $m_s=150$  MeV, the strangelet can be stable only for  $B^{1/4} \lesssim 153$  MeV at  $T=0$ ,  $B^{1/4} \lesssim 151$  MeV at  $T=15$  MeV, and  $B^{1/4} \lesssim 145$  MeV at  $T=30$  MeV. For  $B^{1/4}=145$  MeV, the strangelet is stable only for  $T \lesssim 30$  MeV with  $m_s=150$  MeV, and  $T \lesssim 42$  MeV with  $m_s=0$ . This can impose important restrictions on the possible existence of hot strange quark matter, *e.g.* strange stars in astrophysics. From the fact that ordinary nuclei are composed of nucleons instead of up-down quark matter we can obtain a lower limit ( $B^{1/4} \gtrsim 145$  MeV) of the bag constant



[15]. For the most extreme choice of parameters, *i.e.*  $B^{1/4}=145$  MeV and  $m_s=0$  (see dashed line in Fig. 4), we find that strange quark matter at a temperature  $T \gtrsim 42$  MeV cannot exist stable.

The critical baryon number  $A_{cri}$ , below which the strangelet cannot be stable, is an increasing function of  $T$ ,  $B$  and  $m_s$ . For  $m_s=150$  MeV and  $B^{1/4}=145$  MeV, the critical baryon number is about  $A_{cri} \simeq 25$  at  $T=0$ , and  $A_{cri} \simeq 60$  at  $T=20$  MeV.

The strangeness fraction of the strangelet,  $f_s$ , is found to increase slowly with the increase of temperature  $T$  or baryon number  $A$  (except for  $A \lesssim 100$ ). However,  $f_s$  as an increasing function of  $B^{1/4}$  and a decreasing function of  $m_s$ , is sensitive to the values of  $B^{1/4}$  and  $m_s$ . For  $m_s=150$  MeV and  $B^{1/4}=145$  MeV, the typical values of  $f_s$  are about 0.4-0.7. In terms of the simple relationship  $Z/A = (1 - f_s)/2$ , the charge-to-baryon-number ratio  $Z/A$  has typical values about 0.15-0.3, for  $m_s=150$  MeV and  $B^{1/4}=145$  MeV.

Finally the averaged radius per baryon,  $R/A^{1/3}$ , is a slowly increasing function of  $T$  or  $m_s$ , and a slowly decreasing function of  $A$ , whereas it decreases fast with the increase of  $B^{1/4}$ . For  $m_s=150$  MeV,  $B^{1/4}=145$  MeV,  $R/A^{1/3}$  ranges from 0.9 to 1.1 fm.

To conclude, we have shown in the present work that liquid drop model including finite size effects provides a successful description of properties of strangelets at zero and finite temperature, and allows studies for a wide range of parameters. It is possible to carry out further explorations of phase structure, phase evolution, and possible survival of strangelets in ultrarelativistic heavy ion collisions within the framework of liquid drop model.

## ACKNOWLEDGMENTS

The authors would like to thank Prof. R. K. Su and Dr. S. Gao for fruitful discussions. Y.B.H. is grateful to Prof. Jes Madsen for helpful correspondence.

## APPENDIX:

Eqs. (11) and (12) are given by minimizing the free energy

$$F = \sum_{i=q,s} (\Omega_i + N_i \mu_i) + BV, \quad (\text{A1})$$

with respect to  $V$ ,  $N_q$  and  $N_s$ , under the constraint

$$\sum_i N_i = 3A \quad (\text{A2})$$

for fixed baryon number  $A$ . For the sake of simplicity we omit the surface and curvature terms in  $F$  in the following derivations.

Constructing an auxiliary function

$$F' = \sum_{i=q,s} \{ \Omega_i(V, \mu_i(V, N_i)) + N_i \mu_i(V, N_i) \} + BV + \lambda \left( \sum_{i=q,s} N_i - 3A \right), \quad (\text{A3})$$

we can derive the constrained minimum from

$$\left( \frac{\partial F'}{\partial V} \right)_{N_i} = 0, \quad (\text{A4})$$

and

$$\left( \frac{\partial F'}{\partial N_i} \right)_V = 0. \quad (\text{A5})$$

Since  $(\partial \Omega_i / \partial \mu_i)_V = -N_i$ , Eq. (A4) leads to

$$\left( \frac{\partial F'}{\partial V} \right)_{N_i} = \sum_i \left\{ \left( \frac{\partial \Omega_i}{\partial V} \right)_{\mu_i} + \left( \frac{\partial \Omega_i}{\partial \mu_i} \right)_V \left( \frac{\partial \mu_i}{\partial V} \right)_{N_i} + N_i \left( \frac{\partial \mu_i}{\partial V} \right)_{N_i} \right\} + B = 0, \quad (\text{A6})$$

or

$$\sum_i \left( \frac{\partial \Omega_i}{\partial V} \right)_{\mu_i} + B = 0, \quad (\text{A7})$$

which is Eq. (11).

From Eq. (A5) we obtain

$$\left( \frac{\partial F'}{\partial N_i} \right)_V = \left( \frac{\partial \Omega_i}{\partial \mu_i} \right)_V \left( \frac{\partial \mu_i}{\partial N_i} \right)_V + \mu_i + N_i \left( \frac{\partial \mu_i}{\partial N_i} \right)_V + \lambda = 0, \quad (\text{A8})$$

or

$$\mu_i + \lambda = 0, \quad (\text{A9})$$

which implies

$$\mu_q = \mu_s. \quad (\text{A10})$$

This is Eq. (12).

## REFERENCES

- [1] E. Witten, Phys. Rev. D **30**, 272 (1984).
- [2] E. Farhi and R.L. Jaffe, Phys. Rev. D **30**, 2379 (1984).
- [3] J. Madsen, Phys. Rev. Lett. **61**, 2909 (1988).
- [4] C. Alcock and A. Olinto, Ann. Rev. Nucl. Part. Sci. **38**, 161 (1988).
- [5] C. Alcock, E. Farhi and A. Olinto, Phys. Rev. Lett. **57**, 2088 (1986).
- [6] P. Haensel, B. Paczynski and P. Amsterdamski, Astrophys. J. **375**, 209 (1991).
- [7] C. Greiner, P. Koch and H. Stöcker, Phys. Rev. Lett. **58**, 1825 (1987); Phys. Rev. D **44**, 3517 (1991).
- [8] J. Barrette *et al.* , Phys. Lett. B **252**, 550 (1990); M. Aoki *et al.* , Phys. Rev. Lett. **69**, 2345 (1992); K. Borer *et al.* , Phys. Rev. Lett. **72**, 1415 (1994).
- [9] C. Greiner, D.H. Rischke, H. Stöcker and P. Koch, Phys. Rev. D **38**, 2797 (1988).
- [10] E.P. Gilson and R.L. Jaffe, Phys. Rev. Lett. **71**, 332 (1993).
- [11] J. Madsen, Phys. Rev. D **50**, 3328 (1994).
- [12] H. Reinhardt and B.V. Dang, Phys. Lett. B **202**, 133 (1988); T. Chmaj and W. Słominski, Phys. Rev. D **40**, 165 (1989).
- [13] S. Chakrabarty, Phys. Rev. D **48**, 1409 (1993).
- [14] J. Madsen, Phys. Rev. Lett. **70**, 391 (1993).
- [15] J. Madsen, Phys. Rev. D **47**, 5156 (1993).
- [16] R. Balian and C. Bloch, Ann. Phys. **60**, 401 (1970); T.H. Hansson and R.L. Jaffe, Ann. Phys. **151**, 204 (1983).
- [17] M.S. Berger and R.L. Jaffe, Phys. Rev. C **35**, 213 (1987); **44**, 566(E) (1991).

[18] R. Balian and C. Bloch, Ann. Phys. **64**, 271 (1970).

## FIGURE CAPTIONS

Fig. 1. Free energy per baryon  $F/A$  as a function of the strangeness fraction  $f_s$  with (dashed lines) and without (full lines) Coulomb corrections, at temperature  $T=0$  (upper two curves) and  $T=30$  MeV (lower two curves), for strangelets with a baryon number  $A=100$ , with  $m_s=150$  MeV and  $B^{1/4}=145$  MeV.

Fig. 2.(a)Internal energy per baryon  $E/A$ , (b)strangeness fraction  $f_s$ , (c)charge-to-baryon-number ratio  $Z/A$ , and (d)averaged radius per baryon  $R/A^{1/3}$  as a function of temperature  $T$ , for  $A=20$  (full lines) and  $A=100$  (dashed lines), with  $m_s=150$  MeV and  $B^{1/4}=145$  MeV.

Fig. 3.(a)Internal energy per baryon  $E/A$ , (b)strangeness fraction  $f_s$ , (c)charge-to-baryon-number ratio  $Z/A$ , and (d)averaged radius per baryon  $R/A^{1/3}$  as a function of baryon number  $A$ , at temperature  $T=0$  (full lines) and  $T=30$  MeV (dashed lines), with  $m_s=150$  MeV and  $B^{1/4}=145$  MeV.

Fig. 4. Critical baryon number  $A_{cri}$  as a function of temperature  $T$ , for two different values of  $m_s$ ,  $m_s=150$  MeV (full line) and  $m_s=0$  (dashed line), with  $B^{1/4}=145$  MeV.

Fig. 5.(a)Internal energy per baryon  $E/A$ , (b)strangeness fraction  $f_s$ , (c)charge-to-baryon-number ratio  $Z/A$ , and (d)averaged radius per baryon  $R/A^{1/3}$  as a function of bag constant  $B^{1/4}$ , for strangelets with baryon number  $A=50$ , at temperature  $T=0$  (full lines) and  $T=30$  MeV (dashed lines), with  $m_s=150$  MeV.

Fig. 6. Critical baryon number  $A_{cri}$  as a function of bag constant  $B^{1/4}$ , for strangelets at temperature  $T=0$  (full line),  $T=15$  MeV (dot-dashed line), and  $T=30$  MeV (dashed line), with  $m_s=150$  MeV.

Fig. 7.(a)Internal energy per baryon  $E/A$ , (b)strangeness fraction  $f_s$ , (c)charge-to-baryon-number ratio  $Z/A$ , and (d)averaged radius per baryon  $R/A^{1/3}$  as a function of strange quark mass  $m_s$ , for strangelets with a baryon number  $A=50$ , at temperature  $T=0$  (full lines) and  $T=30$  MeV (dashed lines), with  $B^{1/4}=145$  MeV.

Fig. 8. Critical baryon number  $A_{cri}$  as a function of strange quark mass  $m_s$ , for strangelets

at temperature  $T=0$  (full line)  $T=15$  MeV (dot-dashed line) , and  $T=30$  MeV (dashed line), with  $B^{1/4}=145$  MeV.

Fig. 1

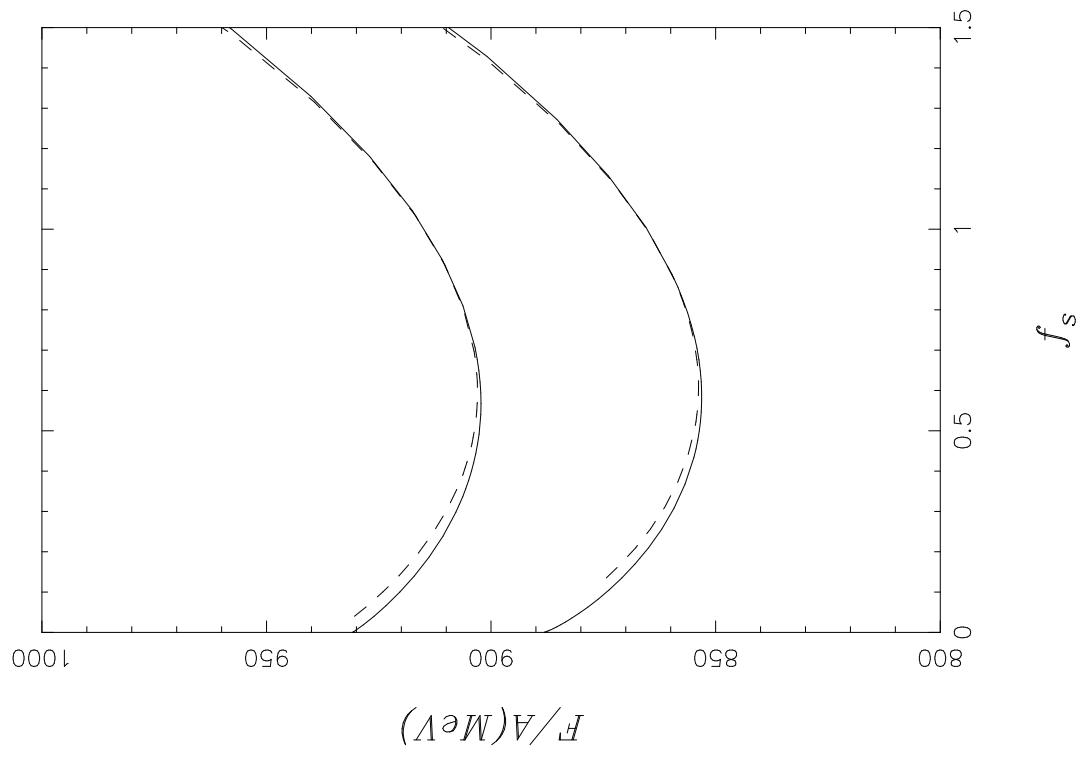


Fig. 2

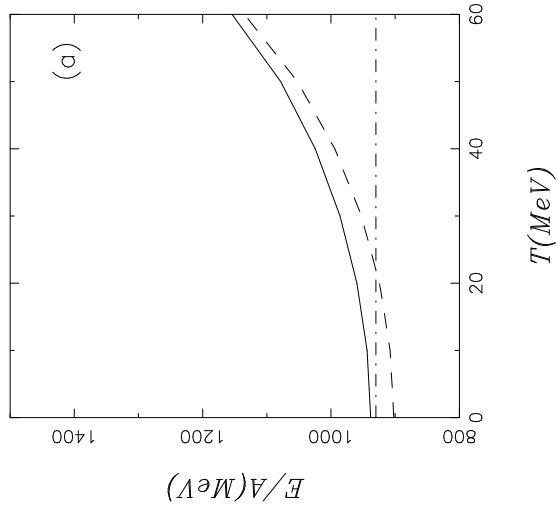


Fig. 2

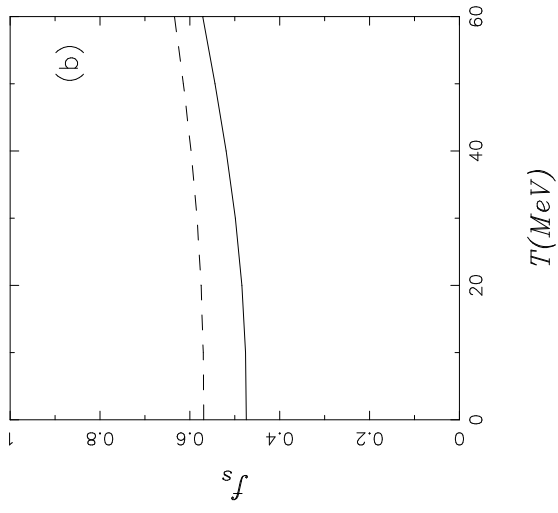


Fig. 2

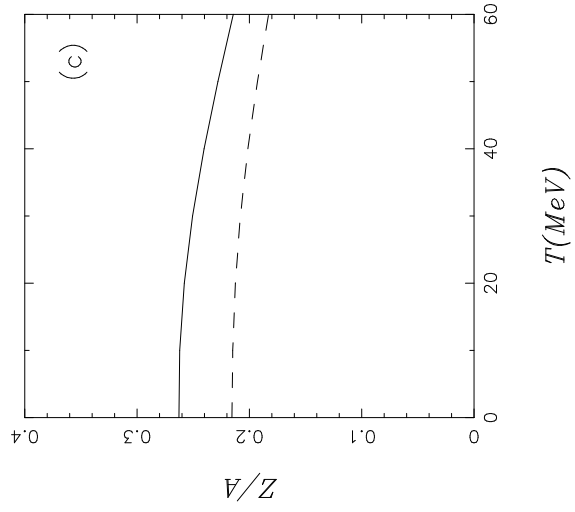


Fig. 2

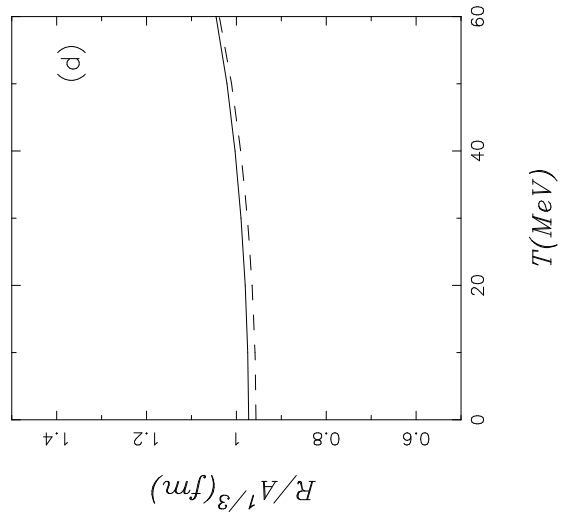




Fig. 3

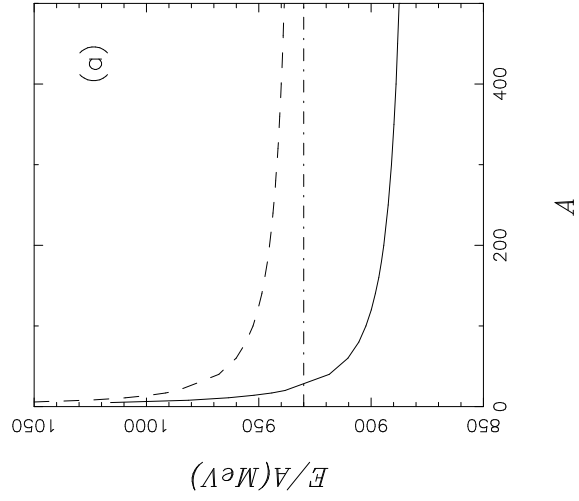


Fig. 3

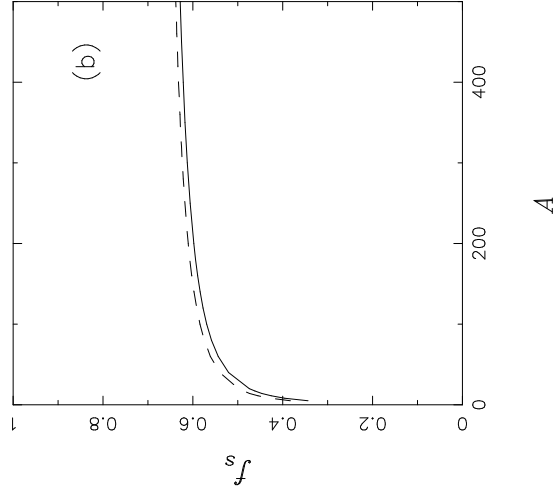


Fig. 3

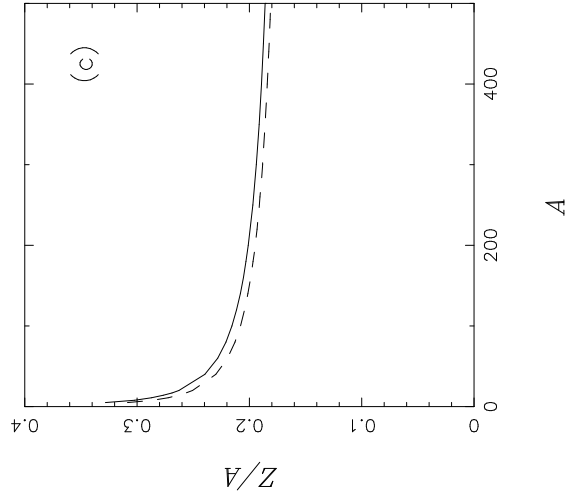


Fig. 3

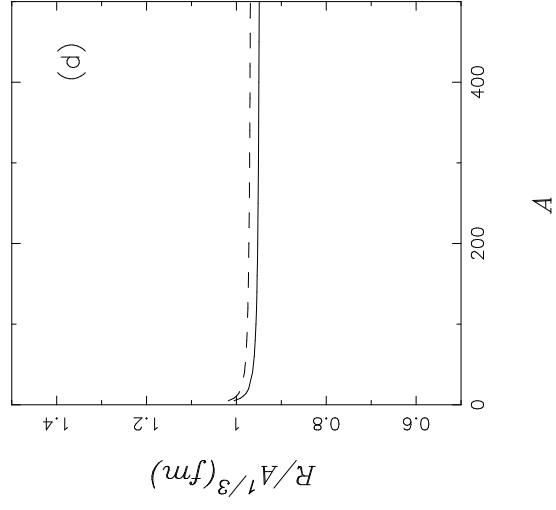


Fig. 4

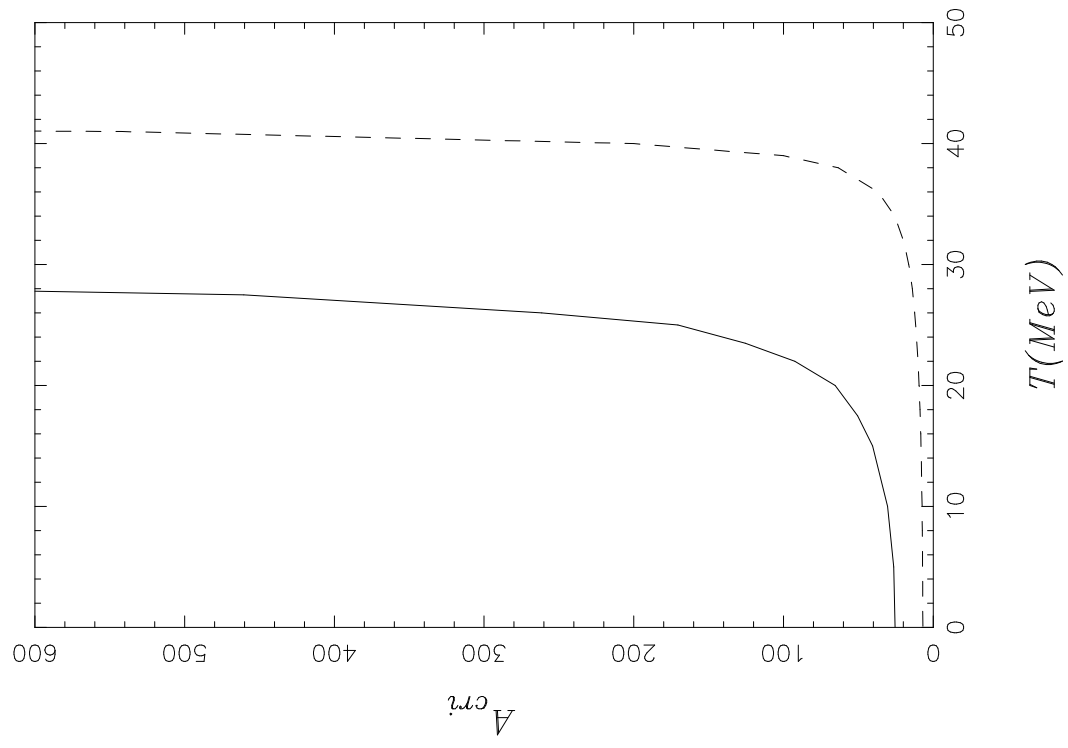


Fig. 5

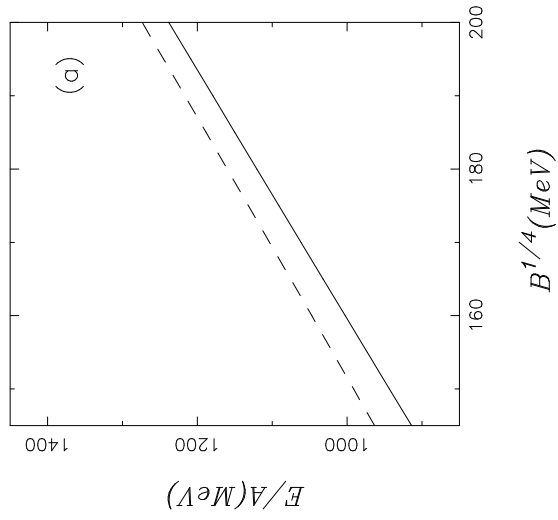


Fig. 5

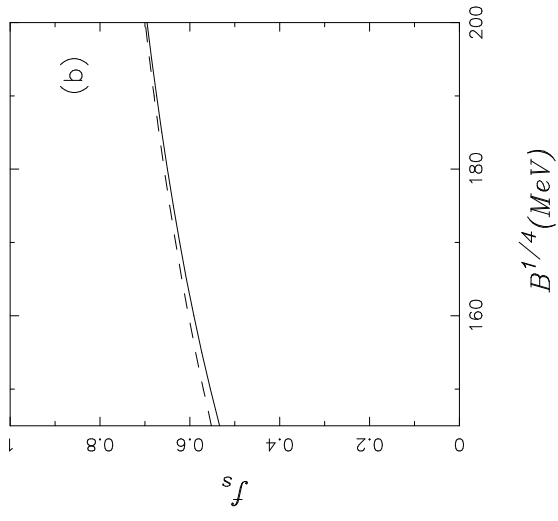


Fig. 5

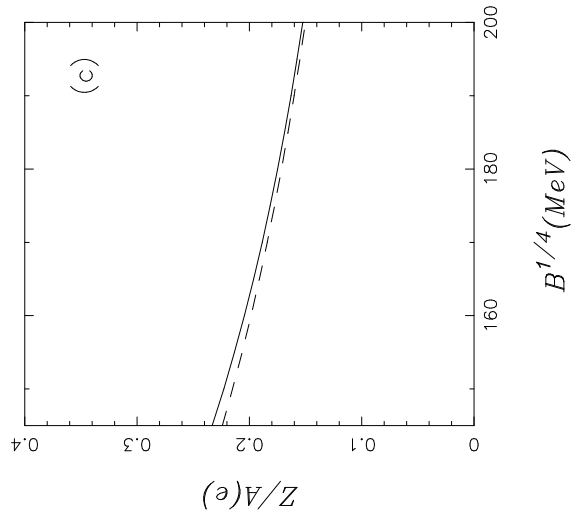


Fig. 5

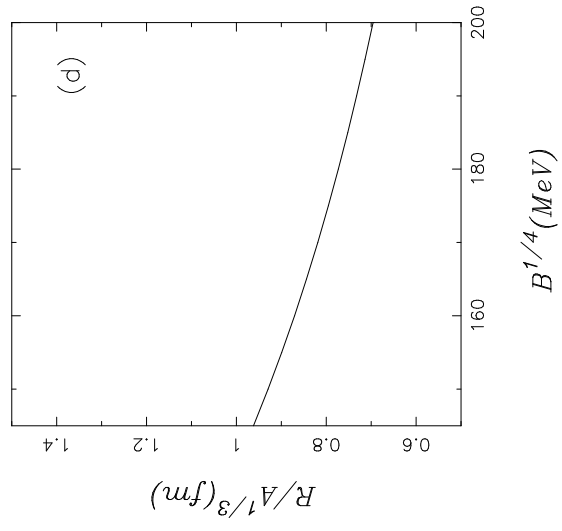


Fig. 6

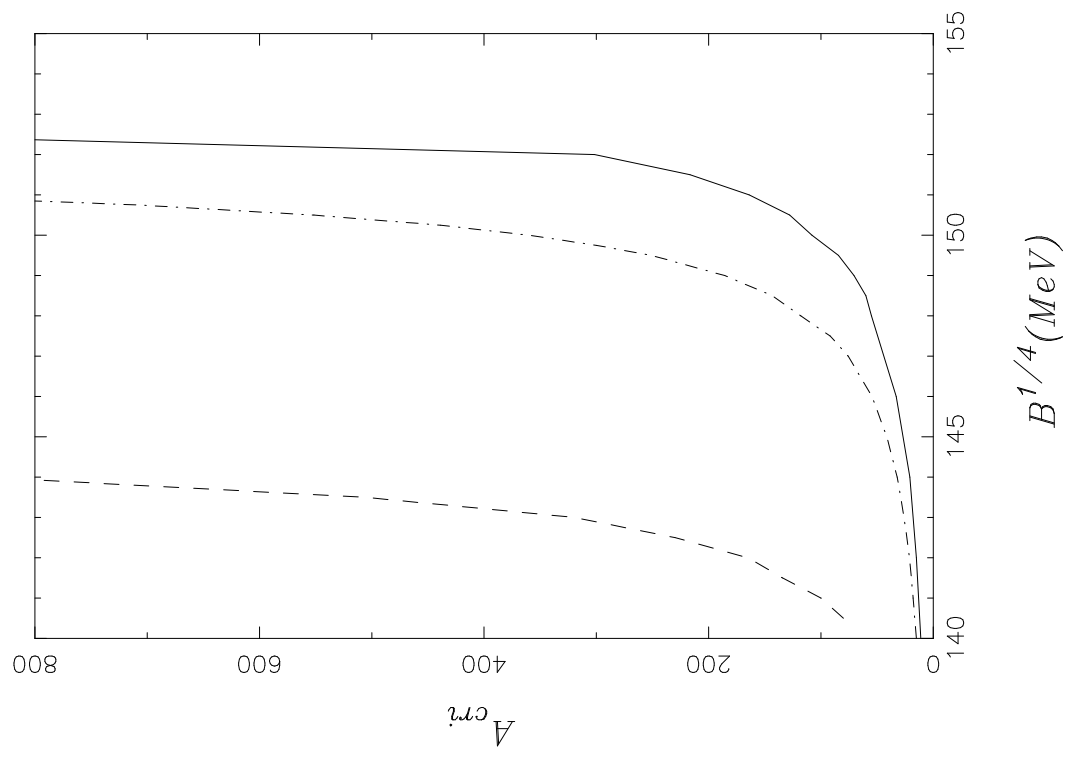


Fig. 7

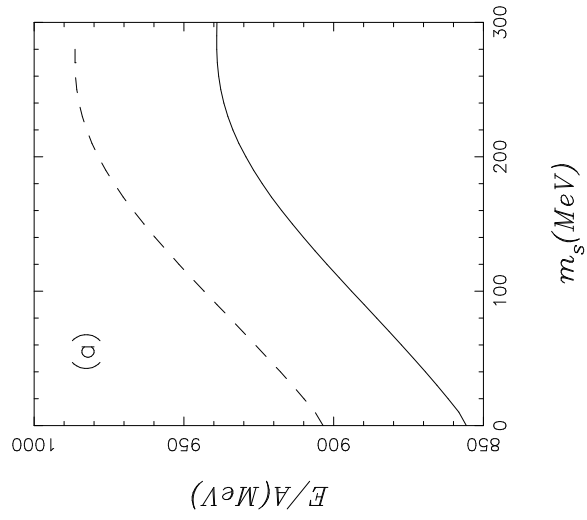


Fig. 7

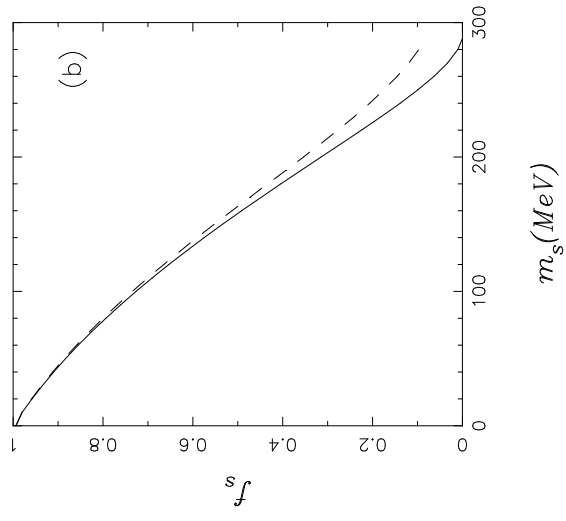


Fig. 7

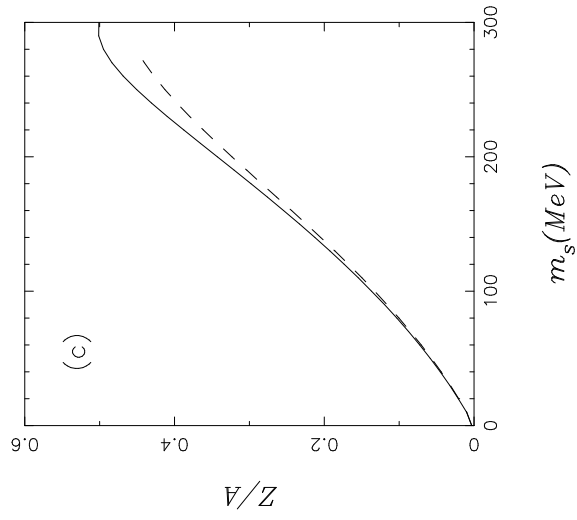


Fig. 7

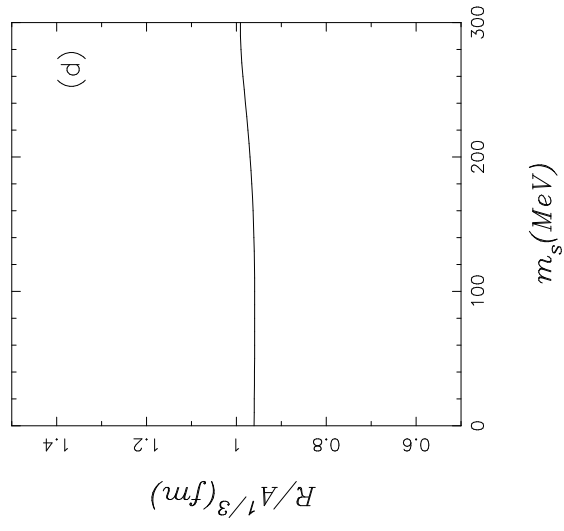


Fig. 8

